

Introduction

Subduction thrust systems are important to understand because they generate the world's largest, most devastating tsunamis. The Hikurangi subduction zone, with the trench just offshore of Gisborne, North Island, New Zealand, has been the site of episodic slow slip events (Wallace et al., 2016). In an effort to help better define the faulting parameters at the plate interface and in the overriding plate, we used first arrival polarity data to determine seismic focal mechanisms for subduction zone earthquakes recorded during the Hikurangi Ocean Bottom Investigation of Tremor and Slow Slip (HOBITSS) project. A better understanding of the relationship between slow slip events and earthquake source parameters is needed to determine the likelihood of damaging earthquakes and tsunamis along the Hikurangi margin.

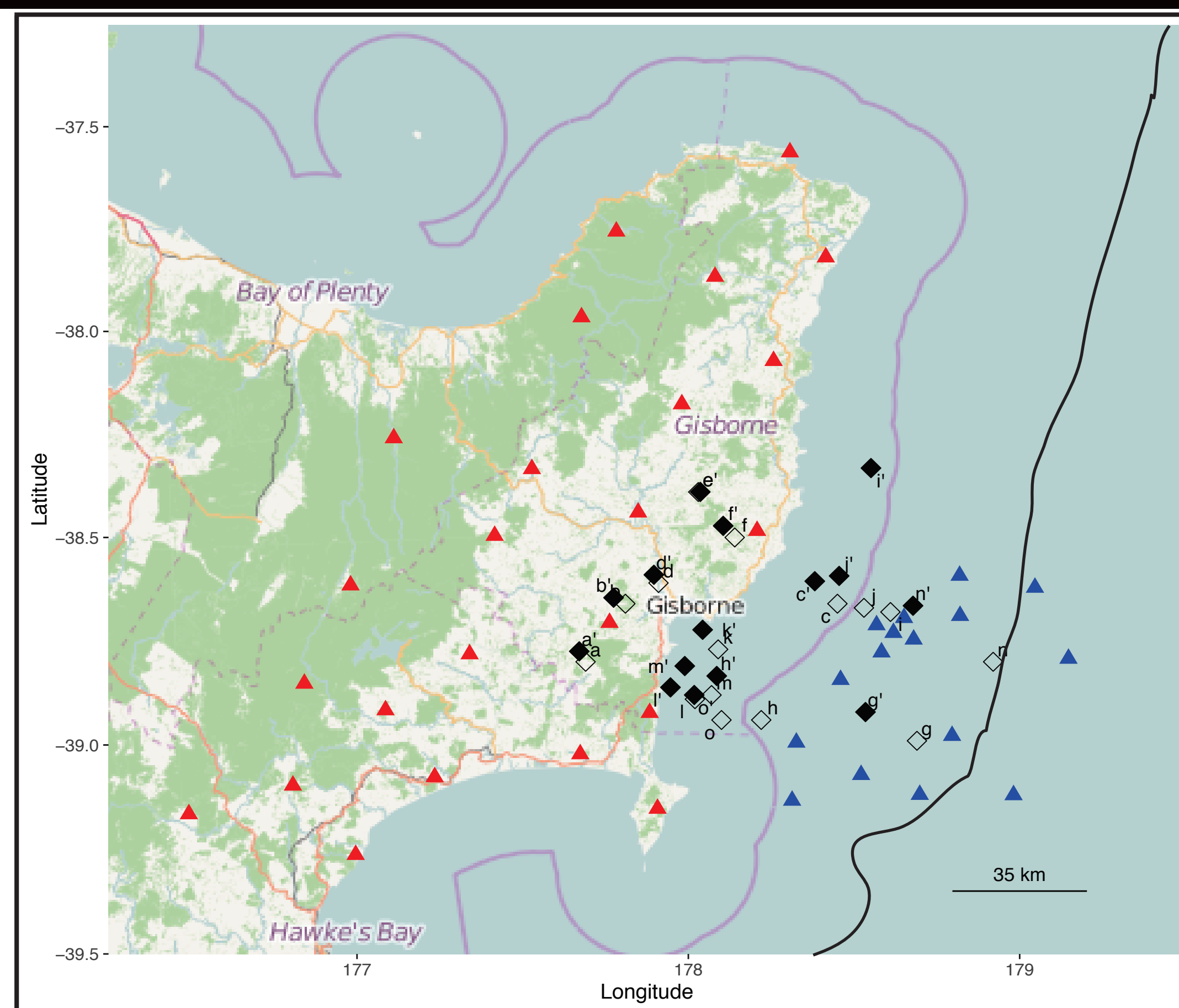


Figure 1. Map of the coastal region of Gisborne, North Island, New Zealand. The red triangles mark the locations of the GeoNet land stations used in this study. Blue triangles are the ocean bottom seismometers deployed during the HOBITSS experiment. Black diamonds are epicenters of the events before and after relocation. See Table 1 for labels.

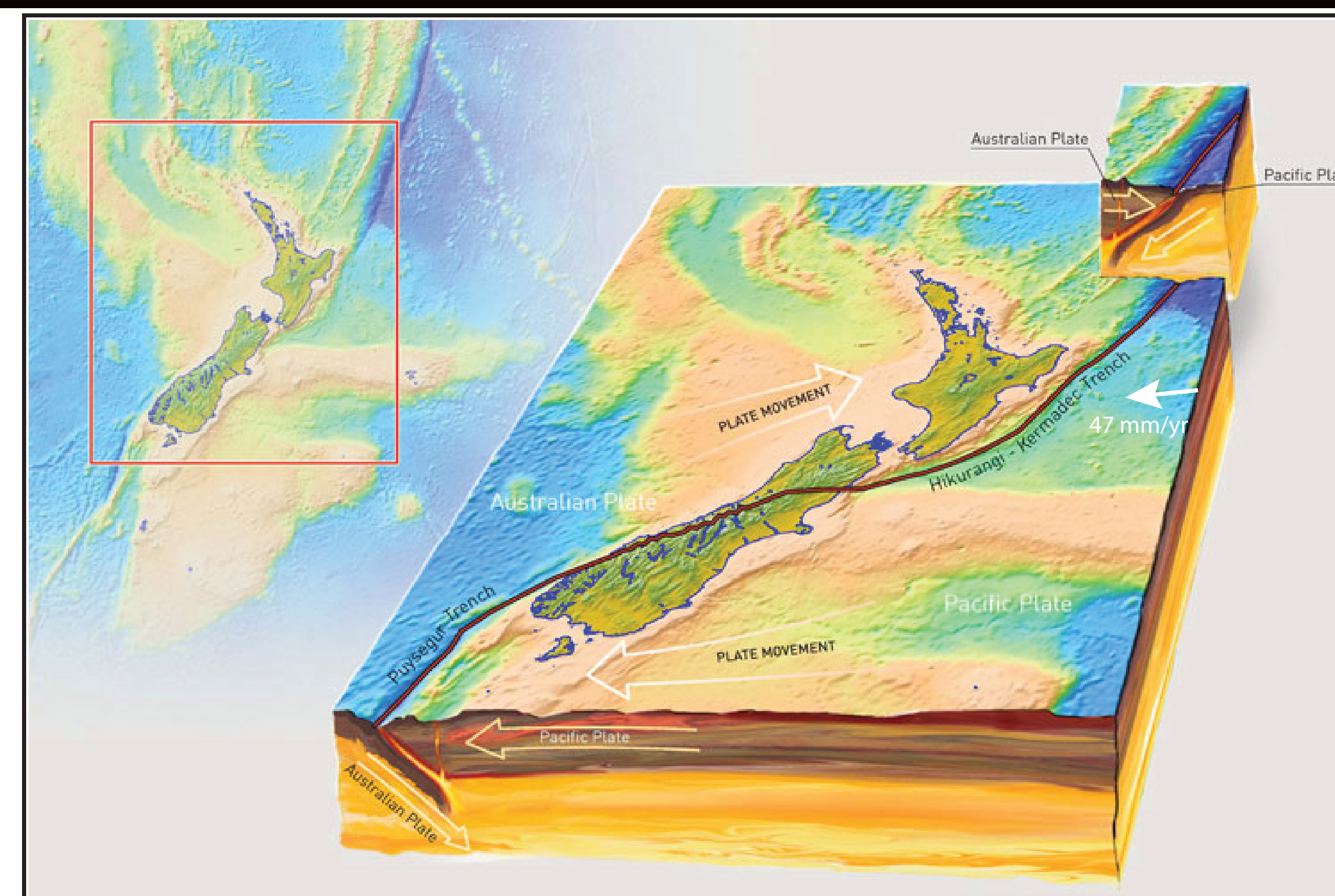


Figure 2. Map and block section showing the tectonic setting of New Zealand (www.aucklandmuseum.com). The Hikurangi Trench lies at the southern end of the Kermadec subduction zone. At our study site off the east coast of the northern North Island, the Hikurangi Plateau, a large igneous province that rides on top of the Pacific Plate, undergoes westward subduction beneath the Australian Plate at a rate of 47 mm/yr. The buoyancy of this feature provides an excellent opportunity to study the subduction thrust since it causes the plate interface to lie above a depth of 15 km just offshore of Gisborne (Harris et al., 2016).

Methods

First P-wave arrivals were picked in the Antelope environmental monitoring software and used to relocate the earthquakes with the LocSAT algorithm and the iasp91 velocity model (Figure 3). Once the polarity data and travel time information were gathered, we used the TauP Toolkit and the iasp91 velocity model to determine takeoff angles for our first arrivals. We used the FOCMEC software written by Snoko (2003) to plot arrivals at each station onto half-sphere stereographic projections. The algorithm then uses a grid-search approach to find the nodal plane solutions with the best fit to the data. Solution quality is determined by the lowest RMS value (<10.5="A", 10.5-25="B", and >25="F").

Results

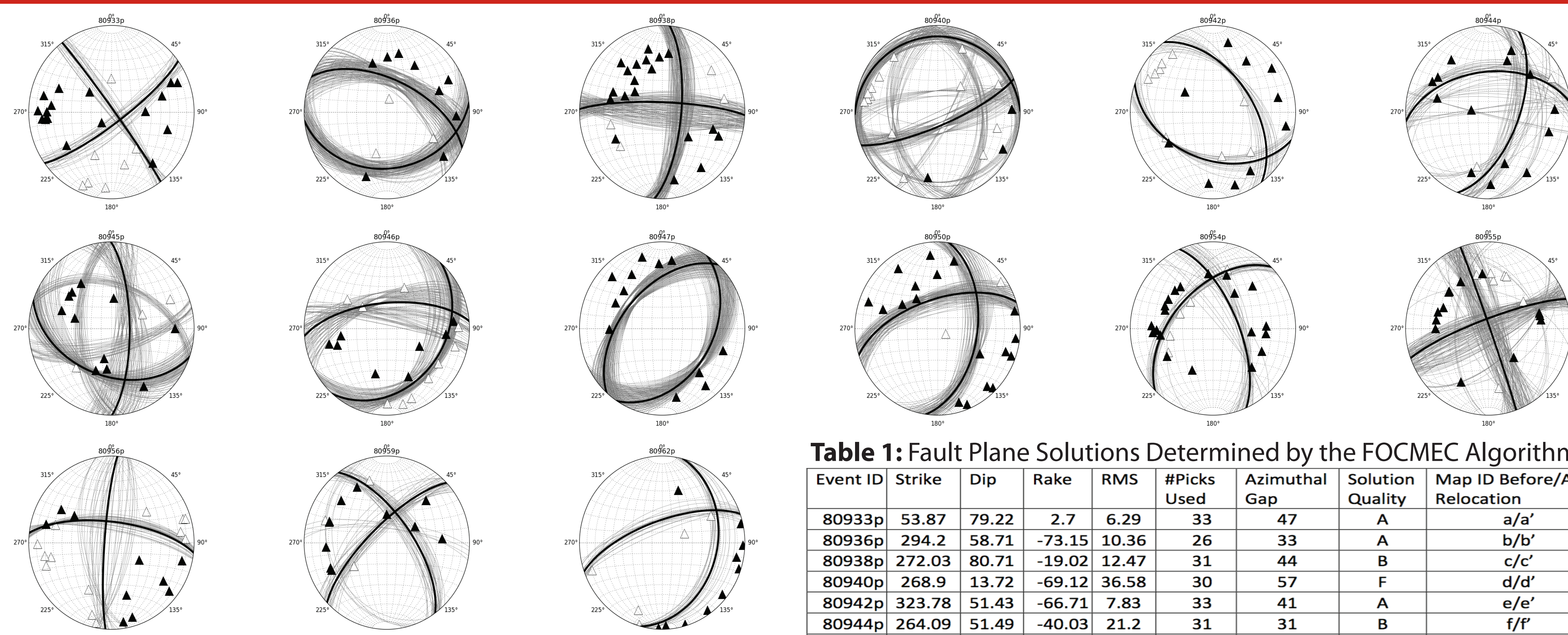
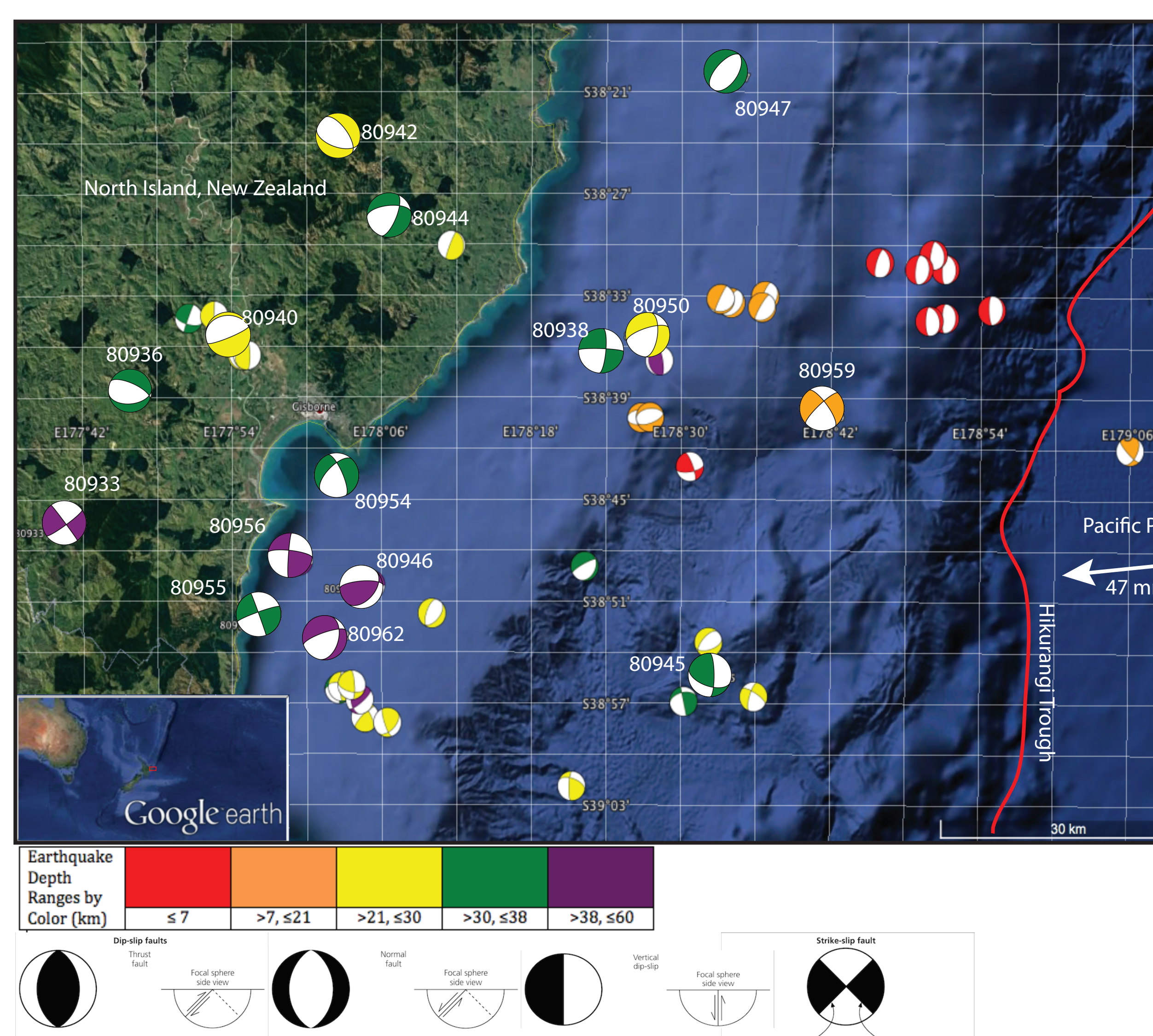


Figure 4 (Above). Focal mechanism plots for the 15 earthquakes used in this study. The triangles represent the first motions experienced by seismic stations surrounding the event. Those plotted in black are arrivals with a positive polarity (compressional) and those in white have a negative polarity (dilatational). Each gray line is a potential nodal plane solution determined by the FOCMEC software, with the lowest RMS solutions plotted as thick black lines.

Table 1: Fault Plane Solutions Determined by the FOCMEC Algorithm

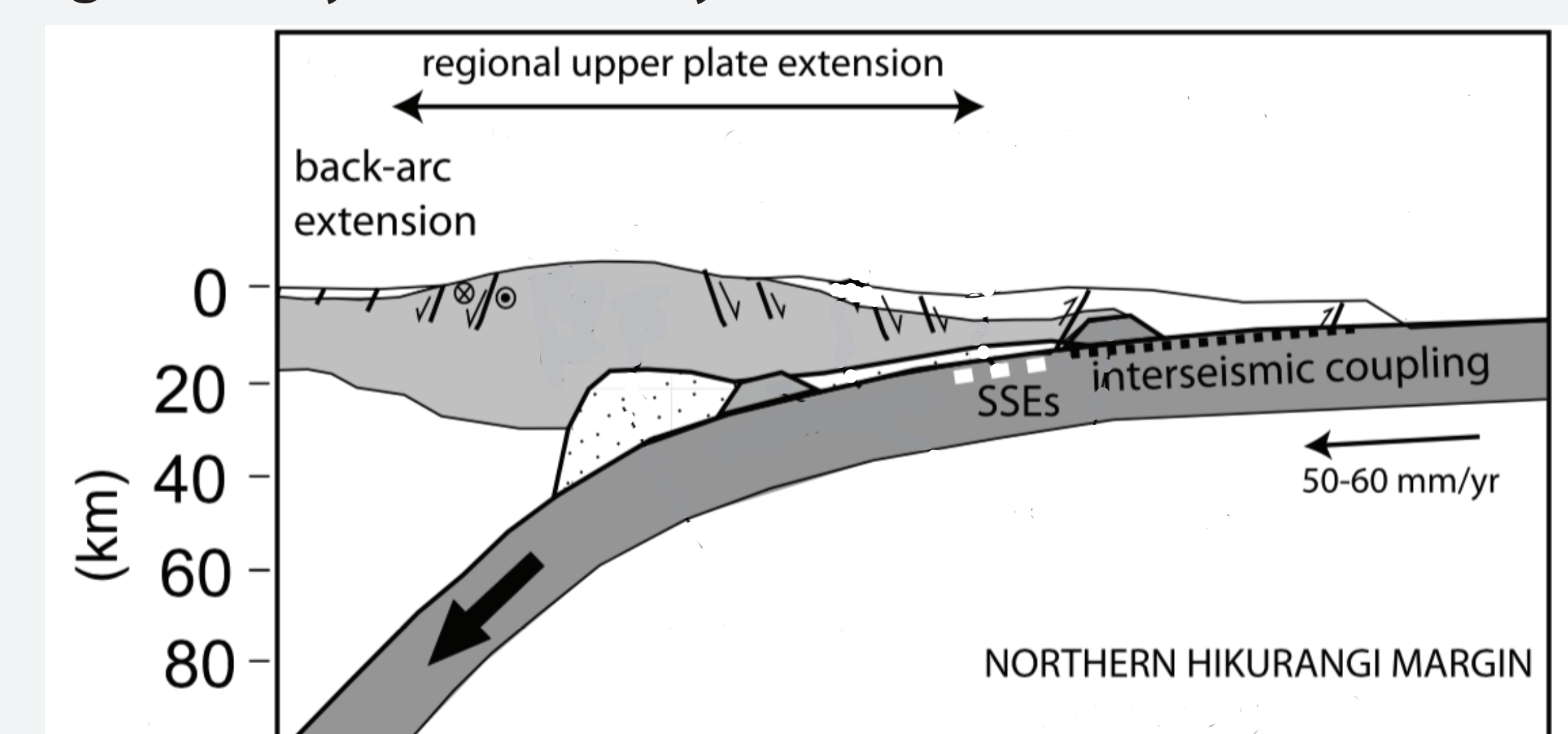
Event ID	Strike	Dip	Rate	RMS	#Picks Used	Azimuthal Gap	Solution Quality	Map ID Before/After Relocation
80933p	53.87	79.22	2.7	6.29	33	47	A	a/a'
80936p	294.2	58.71	-73.15	10.36	26	33	A	b/b'
80938p	272.03	80.71	-19.02	12.47	31	44	B	c/c'
80940p	268.9	13.72	-69.12	36.58	30	57	F	d/d'
80942p	323.78	51.43	-66.71	7.83	33	41	A	e/e'
80944p	264.09	51.49	-40.03	21.2	31	31	B	f/f'
80945p	109.12	44.19	26.26	41.15	29	60	F	g/g'
80946p	40.87	32.03	50.53	10.64	26	72	B	h/h'
80947p	222.35	50.84	-84.17	55.73	18	101	F	i/i'
80950p	252.08	62.42	-46.37	7.08	28	75	A	j/j'
80954p	224.49	51.01	-32.37	5.74	37	75	A	k/k'
80955p	250.04	81.01	-1.57	19.92	30	38	B	l/l'
80956p	276.57	70.31	7.25	4.82	45	65	A	m/m'
80959p	226.23	73.25	-25.69	23.13	28	114	B	n/n'
80962p	250.58	69.4	-62.54	5.86	24	81	A	o/o'

Figure 5 (Right). Map with earthquake focal mechanisms colored by depth and plotted according to their epicentral locations along the Hikurangi subduction zone. Labeled beach balls correspond to the arrival-based solutions featured above. Unlabeled diagrams represent GeoNet focal mechanisms found using regional moment tensor analysis (data available at info.geonet.org.nz). Focal mechanisms provide insights about the geometry of faulting at an earthquake source. Of the two possible planes in a solution, only one is truly representative of the fault that ruptured. The depth and regional geology must be considered alongside the beach balls during interpretation. Accompanying this map are both a key that indicates the depth ranges in which the plotted events were located, and a figure modified from Stein and Wysession (2003) that illustrates how various types of faults are represented as beach balls.



Discussion

Resolvable patterns exist in our lower-hemisphere plots that help to define the geometry of faulting during each of our selected earthquakes. However, when we compare the results of our event relocations to the New Zealand national seismic catalogue, we see notable differences in the depth determinations and epicentral locations. This is likely an artifact of several things. First, the locations of offshore events made by GeoNet may have increased uncertainty since the events are outside of their network. Second, our locations may lack the desired precision because of the velocity model that we used. GeoNet uses velocity models that have been developed to represent New Zealand at the regional scale, whereas the iasp91 model that we used describes the global velocity structure of the Earth. Although many of our relocations might be improvements to previous values, further analysis is required before any faulting parameters should be drawn from our results with certainty. Below is a schematic diagram illustrating the probable faulting geometry of our study area (Wallace et al., 2009).



Conclusion

The ocean bottom seismometers deployed during the HOBITSS experiment provide a new opportunity to investigate earthquakes along the Hikurangi margin. Our analysis yielded 12 fault plane solutions with a reasonable fit. However, the iasp91 velocity model does not provide the desired resolution for a study of this scale. A regional velocity model will be used to add constraints to our focal mechanisms before geological interpretation is made.

Acknowledgements

This material is based upon work supported by the National Science Foundation under Award No. EAR 1261833. Additional support was provided by ExxonMobil, UNAVCO, and the RESESS program. Special thanks go out to Jacky Baughman, Sarah Evans, Rolf Norgaard, and Will Yeck for their assistance in developing this presentation. Thanks also to Aisha Morris, Melissa Weber, and my fellow RESESS interns for their help and encouragement this summer.

References: Harris, R., L. Wallace, S. Webb, Y. Ito, K. Mochizuki, H. Ichihara, S. Henrys, A. Trehu, S. Schwartz, A. Sheehan, D. Saffer, and R. Lauer (2016), Investigation of Shallow Slow Slip Offshore of New Zealand, *Eos*, 97, doi:10.1029/2016EO021603; Ristau, J. (2008), Implementation of routine regional moment tensor analysis in New Zealand, *Seismol. Res. Lett.*, 79(3), 400, doi:10.1785/gssrl.79.3.400.; Snoko, J. A. (2003), FOCMEC: focal mechanism determinations, *Int. Handb. Earthq. Eng. Seismol.*, 85, 1B22.; Stein, S., and M. Wysession (2003), *An introduction to seismology, earthquakes, and earth structure*, Blackwell Pub, Malden, MA.; Wallace, L. M., S. C. Webb, Y. Ito, K. Mochizuki, R. Hino, S. Henrys, S. Y. Schwartz, and A. F. Sheehan (2016), Slow slip near the trench at the Hikurangi subduction zone, New Zealand, *Science* (80-), 352(6286), 701B704.; Wallace, L. M. et al. (2009), Characterizing the seismogenic zone of a major plate boundary subduction thrust: Hikurangi Margin, New Zealand, *Geochemistry, Geophysics, Geosystems*, 10(10), doi:10.1029/2009GC002610.

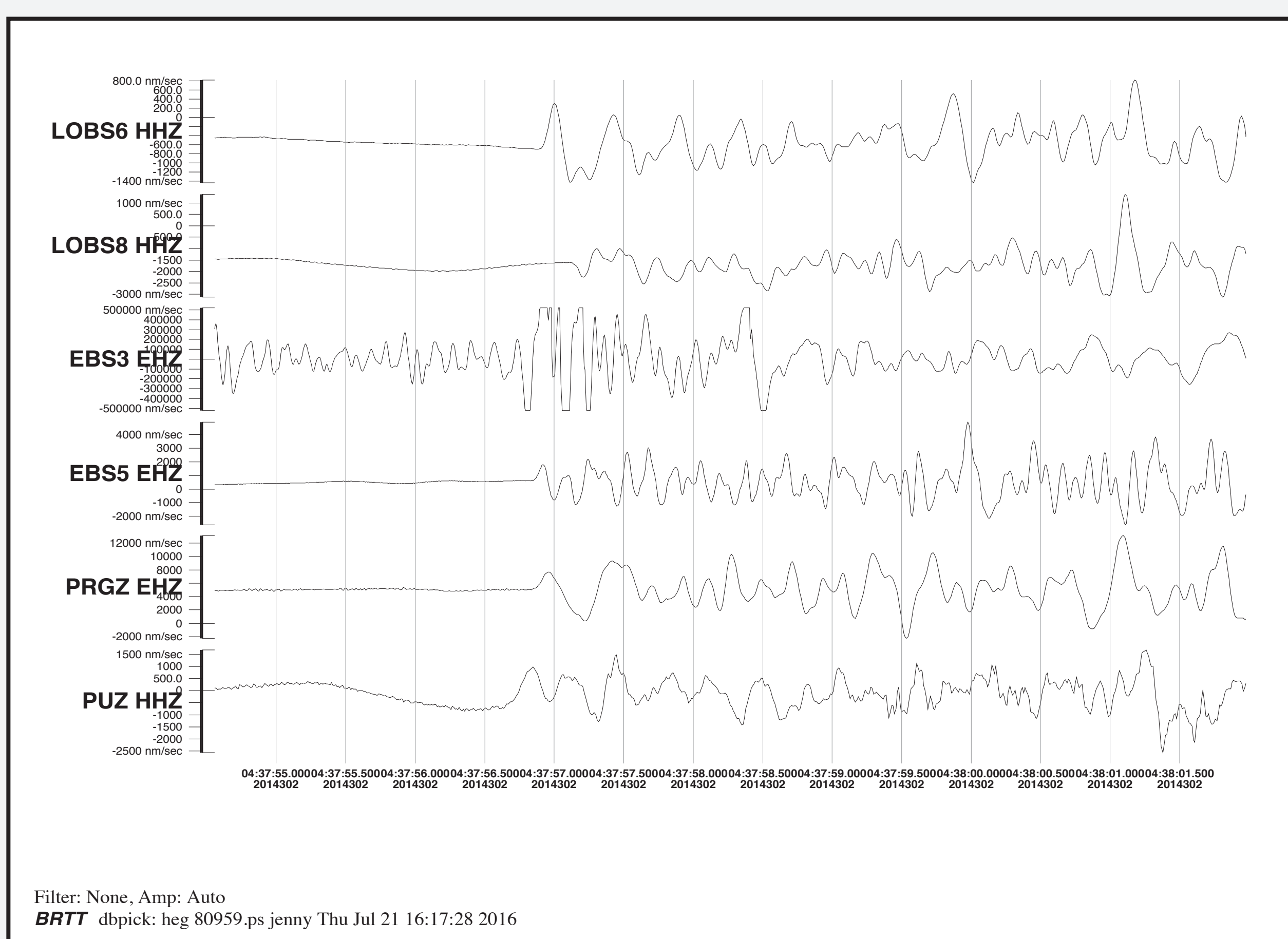


Figure 3. Examples of vertical component waveforms from event 80955. For each earthquake, a waveform must be evaluated at each station featured in Figure 1. Ideally, a P-wave first arrival is assigned either a positive (compressional) or negative (dilatational) polarity. As you can see from station EBS3 in this example, stations often exhibit noisy data or weak first arrivals that prohibit confident polarity assignments. This leaves gaps in the plotted solutions, and ultimately affects where nodal planes are fit.